

V CIRP Conference on Biomanufacturing

# Ultrafast laser micromanufacturing of microfluidic devices

Leonardo Orazi<sup>a,b,\*</sup>, Vincenzina Siciliani<sup>b</sup>, Riccardo Pelaccia<sup>b</sup>, Keltoum Oubellaouch<sup>a</sup>, Barbara Reggiani<sup>a,c</sup>

<sup>a</sup>DISMI – University of Modena and Reggio Emilia, Via Amendola 2, Reggio Emilia 42122, Italy

<sup>b</sup>EN&TECH – University of Modena and Reggio Emilia, Piazzale Europa 1, Reggio Emilia 42124, Italy

<sup>c</sup>INTERMECH – University of Modena and Reggio Emilia, Piazzale Europa 1, Reggio Emilia 42124, Italy

## Abstract

Microfluidic devices play a continuous increasing role in the drugs and nanomedicine production and delivery and in diagnostic kits. Three main classes of materials are employed in manufacturing microfluidic devices: mainly polymers, metals and glasses. The mass production of microfluidic devices is normally based on micro-injection molding of PDMS but there are cases that discourage the use of PDMS such as when incompatible solvents must be used in drug formulation. Moreover, the use of PDMS based systems requires the manufacturing of micro-molds, a time expensive activity that strongly affects the development and the prototyping stage. In this work, the use of UV picosecond laser for the generation of micro-channels on glass surfaces is demonstrated. The surface topography and the geometric characteristics of the features are correlated with the main process parameters providing considerations on the process productivity.

© 2022 The Authors. Published by Elsevier B.V.

This is an open access article under the CC BY-NC-ND license (<https://creativecommons.org/licenses/by-nc-nd/4.0>)

Peer-review under responsibility of the scientific committee of the V CIRP Conference on Biomanufacturing

**Keywords:** Ultrafast laser; UV; picosecond; microfluidic; glass

## 1. Introduction

Microfluidics have recently found wide application in the fields of nanomedicine and nano-pharmaceuticals, which aim to transfer the unique features of nanomaterials into therapeutic products [1]. Specific microfluidic devices for the medical industry are manufactured either for the drug production and delivery, or for the rapid diagnostic kits to test and diagnose diseases [2].

Typical microfluidic systems transport, mix, separate or otherwise process fluids. The geometrical features of these devices range between few  $\mu\text{m}$  to hundreds of  $\mu\text{m}$ . These devices are usually manufactured by micro-injection molding of separate pieces followed by bonding using gluing or welding [3].

Generally, these devices can be made from a variety of materials, including silicon, glass, hydrogel, paper and polymers, each with its advantages and disadvantages. Historically, the first materials for microfluidic device fabrication (as MEMs and microelectronics [4]) were glass and silicon. The chips were made by wet etching and fusion bonding processes. With these processes, the stiffness and the chemical resistivity of the materials required high temperature and pressure conditions in the different phases, super clean environment and the use of lithographic masks and dangerous chemicals; this resulted in an increase of the overall manufacturing cost and consequently a limitation in the use of these materials. Thus, for laboratory research, where a trade-off must be made between easiness of fabrication and device performance, the most widely used materials have become elastomers, particularly polydimethylsiloxane (PDMS) [5]. The latter material is

\* Corresponding author. Tel.: +390522522607; fax: +390522522609.

E-mail address: [leonardo.orazi@unimore.it](mailto:leonardo.orazi@unimore.it)

convenient in fabrication and it can be easily cast with high resolution once micro-molds are generated by photolithography process. However, it is permeable to gases and this can cause water evaporation during the flow and crystallization of the dissolved analytes. PDMS is also transparent in the UV-visible regions, quite chemical inert, low polar, low electrically conductive, elastic and it does not swell in contact with water [4]. In this regard, the solvent compatibility of PDMS were studied [4, 5]. Lee et Al [4] describe the compatibility of PDMS with organic solvents. The study of this compatibility is important in numerous applications, such as bioanalysis in water or organic synthesis in organic solvents. They conclude that PDMS is limited to certain ranges of solvents. For example, it is used in the microreactors fabrication for organic reactions that involves solvents which are compatible with it. However, reactions requiring highly and extremely soluble solvents may require glass or silicon.

In other applications that rely on passive fluid control using capillary forces [6] it has been established that glass for capillary devices possesses advantages for microfluidic applications, thanks to its ability to withstand organic solvents, when compared with the lithographically fabricated PDMS parts. In addition, glass microfluidic devices have excellent other properties such as their thermal stability and the low risk of channel wall deformation thanks to the high hardness of the glass.

Moreover, as mentioned above, the PDMS based systems involves the manufacturing of micro-molds, a time expensive activity that strongly affects the development and the prototyping stage.

In this context, the development of microfabrication and micromanufacturing technologies must enable scalable processes complying with process economy and quality assurance [2].

For example, for the “large-scale” production of the diagnosis kit, where a batch can be made of 100 pieces/devices and the prototyping is a great step, the use of the glass together with the laser potential can be very helpful.

Ultrashort laser ablation is a direct manufacturing technique very suitable for the rapid and precise prototyping of glass microfluidic devices, where the total volume of the ablated material is small. Ultrashort laser irradiation can modify the microchannel surface to create the desired geometry [7–12] and also affect its wettability [13]; but it leaves a certain roughness [14]. The small pulse width exhibits major advantages over longer pulse durations for precision manufacturing processes. Transparent material like glasses and fused silica can interact with visible and near IR laser thanks to multiphoton absorptions, moreover the availability of High Harmonic Generators modules for ultrashort lasers permit to operate in the UV band where absorption is not negligible. The precise control of energy density allows high flexibility in surface structuring and bulk machining to be performed on almost any transparent material. The removal of material without significant transfer of heat into surrounding areas is the most unique advantage of ultrashort laser pulses. [3]

The approach of performing in-bulk process on glass has been followed for microfluidics applications [9, 15], but

probably machining the surface and then closing the channel appears to be the simplest solution; it also improves the accuracy of the created geometries.

Creating the 2D structures instead requires joining the parts. Researchers used several techniques, as laser welding, anodic bonding, adhesive bonding, but they found some disadvantages: in the laser welding the lateral dimension of weld seams determines the minimum size of the areas suitable for welding [7], high power generates large HAZ [12]; the anodic junction between glass and glass requires an intermediate layer [8]; using adhesives has a high risk of glue getting into the microchannels during the bonding process, blocking fluid flow [16] and a further step is required to pump it away. A practical idea is to use a commercially available muffle furnace to join the parts through diffusion bonding. This technique can limit the man hours needed when compared to other bonding techniques [17], but should be accomplished within non-exaggerated time. In this regard, the application of pressure during heat treatment decreases the time required to join the parts and improves the strength of the joint.

In this work, the adopted approach consists in channels machining on the glass surfaces with ultrashort picosecond laser and then sealing them with a glass cover by diffusion bonding, with the help of a weight during the heat treatment. It is demonstrated the possibility of creating complex geometry on the glass surface. After having detected the obtained roughness, it is modified with heat treatment. Finally, to ensure the stability of the device, the diffusion bonding efficiency is evaluated to create, in principle, closed channels.

## 2. Materials and Methods

Recently, different designs have been introduced to simplify the fabrication process using commercially available components, because many limitations exist with the current design of microfluidics device in large-scale production.

The material used in this study is a float-glass, whose constituents and characteristics are presented in Table 1 and Table 2 respectively, as basic components of the device. Starting from the initial slides, these was cut to obtain glass samples of 25x11mm.

Table 1 . Glass constituents

Constituents	%	Constituents	%
SiO <sub>2</sub>	72,3	CaO	8,8
Al <sub>2</sub> O <sub>3</sub>	0,5	K <sub>2</sub> O	0,4
Fe <sub>2</sub> O <sub>3</sub>	0,02	MgO	4,3
Na <sub>2</sub> O	13,3		

Table 2. Glass physical and chemical characteristics

Thickness tolerances [mm]	0,95 – 1,05
Mean refractive index to visible radiation, n	1,5
Density, $\rho$ [kg/m <sup>3</sup> ]	2500
Average coefficient of linear expansion between 20°C and 300°C, $\alpha$ [K <sup>-1</sup> ]	9x10 <sup>-6</sup>
Thermal conductivity, $\lambda$ [W/mK]	1
Young's modulus, E [Pa]	7x10 <sup>10</sup>
Poisson's ratio, $\mu$	0,2
Alkaline resistance	Class 2
Acid resistance	Class 3
Hydrolytic resistance	Class 3

The glass samples were characterized with a differential thermal analysis (DTA) to evaluate the glass transition temperature  $T_g$ , which was found to be about 574°C as shown in Figure 1.

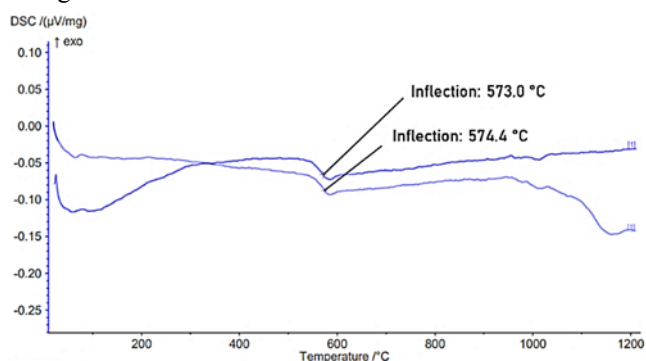


Figure 1. Glass transition temperature evaluation by DTA

A series of heat treatments above the glass transition temperature have been decided to be performed. Going from a temperature of  $T_g+25^\circ\text{C}$  to  $T_g+100^\circ\text{C}$  with a step of  $25^\circ\text{C}$ . This with two objectives:

- to evaluate the change in roughness induced by heat treatments,
- to evaluate the possibility of joining the processed slide with a flat one, to create closed channels as a result of heat treatments.

The thought final device will be in this case composed by a treated sample with the requested geometry, joined by a simple flat glass cover to create the closed channels, as shown in Figure 2. One disadvantage of this thought is that cleaning can only be accomplished by flushing and not by device disassembly.

Grooves has been created on the glass with a picosecond laser facility. The experimental set-up of the ultrafast laser system used is shown in Figure 3. The glass is processed suspended in air over a graphite plate that absorb the most part of transmitted energy. This permits to avoid undesired back reflections and to thermal effects induced by local heating of the supports. The laser is a picosecond amplifier EKSPLA Atlantic 5 which emits three beamlines at 1064, 532 and 355 nm and with pulse duration of about 10 ps. Laser

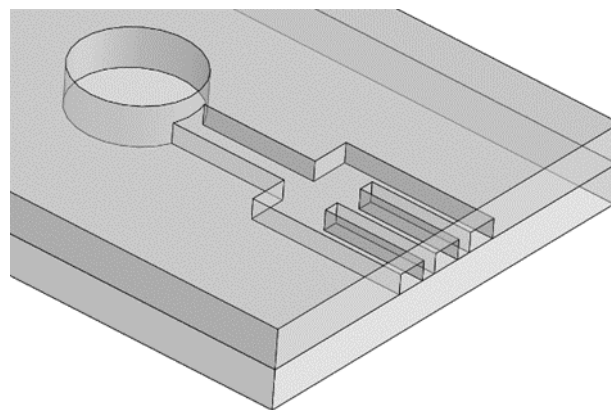


Figure 2. The superimposed glasses for device creation

beam is delivered on the workpiece with a Raylase Superscan 5 galvanometric scanner system with an input diameter of 15 mm. This relatively high aperture coupled with a 104 mm F-theta lens guarantee a  $1/e^2$  spot diameter of 10  $\mu\text{m}$ .

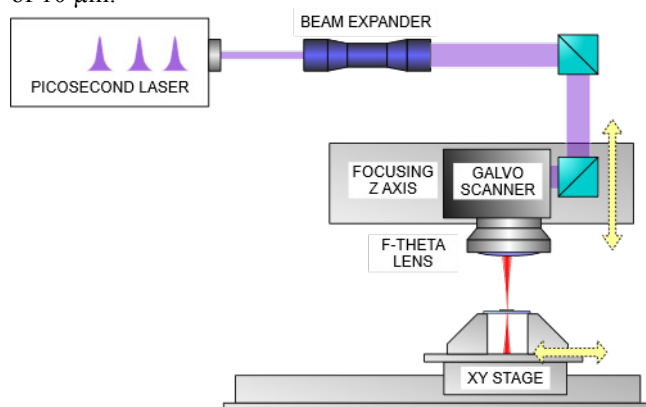


Figure 3. The experimental set-up of the ultrafast laser system used

All the tests were performed using the wavelength of 355nm, a repetition rate of 100 kHz., with a laser power, measured over the workpiece, of 750mW equivalent to pulse energy of 7.5  $\mu\text{J}$ . To ablate the glass surface 4 consecutive passes of overlapping scanlines with a scanning speed of 400mm/s and a scan step of 4  $\mu\text{m}$  was performed as seen in Figure 4 (left). This combination permits to equally distribute and overlap pulses along and between the scanlines.

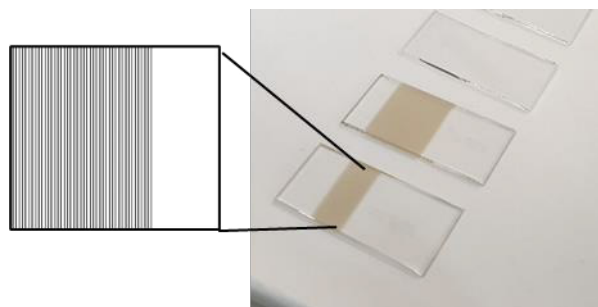


Figure 4. Laser texturing geometry (left) and treated samples (right)

Two versions of the treatment were performed, one to generate surfaces to be evaluated by SEM and AFM and one with a larger treatment area to allow wettability

measurements, as can be seen in Figure 4 (right).

The samples were divided in two sets, to evaluate wettability of untreated (UNT) and Ultrashort laser treated (ULT) samples at different temperatures, as visible in Figure 5.



Figure 5. The different studied cases

The surface morphology of the samples was observed through a Scanning Electron Microscopy, operating mainly in secondary electrons imaging mode.

Surface roughness was measured using an atomic force microscope (AFM).

The wettability of the surfaces was determined through the measurement of distilled and deionized (DD) water contact angles by the sessile drop method. Drop images were acquired at a defined interval of 6s and then analyzed by SCA20 software to evaluate the contact angle. The measurements were performed at room temperature. For each specimen at least 3 drops were generated and their average was calculated.

### 3. Results and Discussion

#### 3.1 Heat Treatment

A Lenton ECF 12/6 muffle oven was used. Heat treatments in ambient air up to 674°C were performed.

Prior to heat treatment and the thermal bonding, the slides were cleaned in an ultrasonic bath to remove any residual ablated material.

The imposed temperature cycle consists of a ramp, from 25°C to the defined temperature for the specific treatment, and a horizontal line in which the temperature of the treatment is maintained for 30 minutes. At the end of each treatment, the oven was allowed to cool down before the next test.

#### 3.2 CA measurements

The results obtained from the contact angle measurements are summarized in Table 3 and Figure 6.

Table 3. Average and Standard Deviation of Water Contact Angle measurement (\*high error)

Sample	CA(°) & Standard Deviation	After 48h	After 96h	After 144h
UNT	58 ± 4			
ULT	48.2 ± 22*	62.4 ± 15 *		

ULT-50	8.1 ± 2		13.5 ± 2.3
ULT25	<5 ± 0		
ULT50	<5 ± 0	10.2 ± 3.9	35.9 ± 9.9*
ULT75	<5 ± 0		
ULT100	14.4 ± 13.9*		
UNT-50	11.8 ± 1.6		27.6 ± 3.6
UNT25	<5 ± 0	12.4 ± 0	27.1 ± 7.8*
UNT50	<5 ± 0	11.0 ± 2.2	32.9 ± 9.2*
UNT75	<5 ± 0		
UNT100	8.4 ± 3.9		

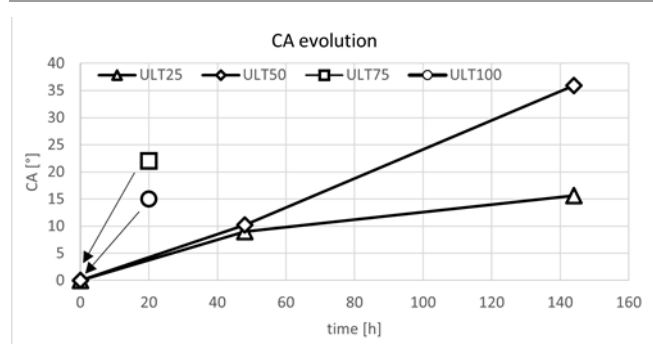


Figure 6. Contact Angle evolution

From untreated material to laser-treated material the wettability increases, which means that the laser makes the material more hydrophilic. It should be mentioned that the material treated in the oven up to 75° above the glass transition temperature, is super-hydrophilic: the deposited droplet slides off and makes CA measurement impossible (Figure 7).

For comparison, the material that only underwent heat treatment in the oven still super-hydrophilic.

Since the measurements were taken immediately after the heat treatment, it is assumed that this cleaned the surface totally from any organic/carbolic residue, thus hydrophobicity.

Few days after the heat treatment, the average water contact angle increased slightly, remaining well within hydrophilicity (Table 3).

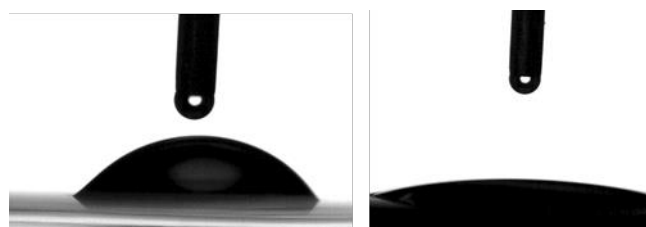


Figure 7. Drop deposited on untreated (left) vs heat treated (right) material

#### 3.3 SEM Image

Figure 8 shows SEM images of the different samples: a) untreated material, b) and c) laser treated in which the groove created on the glass can be seen. The depth obtained is of the order of magnitude of 20 µm.



Figure 8. SEM image of untreated sample (a), laser treated sample in different magnification (b,c)

Figure 9 shows a-b) the laser-treated samples (without heat treatment), c-d) the heat-treated samples at  $T_g+25^\circ\text{C}$ , e-f)  $T_g+50^\circ\text{C}$ , g-h)  $T_g+75^\circ\text{C}$  at two different magnifications to appreciate the resulting microstructure, unvaried in shape by the heat treatment. In conclusion, the microstructure remains similar but enlarged.

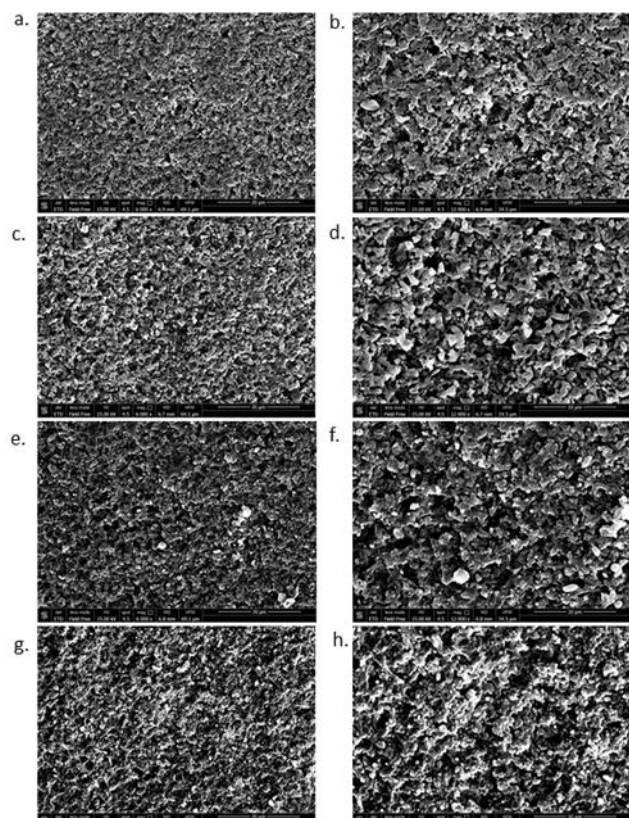


Figure 9. SEM image of laser treated samples (a,b), laser heat treated at  $T_g+25^\circ\text{C}$  (c,d),  $T_g+50^\circ\text{C}$  (e,f),  $T_g+75^\circ\text{C}$  (g,h)

### 3.4 AFM Analysis

AFM analysis obtain images thanks to the interactions generated between the sample and a 'probe'. The images can be related both to the morphology and to the chemical-physical properties of the sample. In this context, morphological characteristics of  $50 \times 50 \mu\text{m}$  areas for different samples were analyzed to have comparable results. The average roughness of the parallel microfluidic channel composed of multi-pass channels was found to be above 2

$\mu\text{m}$ , the heat treatment till does not change a lot this value, while the virgin material presented an average roughness of about  $1 \mu\text{m}$ .

Surface characteristics are in Table 4, in terms of Means Roughness ( $S_a$ ), RMS roughness ( $S_q$ ), Maximum height ( $S_z$ ) and a Surface Ratio defined as Surface Area/Projected area, thus greater than 1. It was found that the roughness decreases with increasing temperature in the oven, but at  $T_g+100^\circ\text{C}$  it starts to increase. In any case, the variation of roughness is very interesting and can be advantageously exploited to create devices.

Table 4. Roughness measurement of the samples (\*high error)

Sample (50x50 $\mu\text{m}$ area)	$S_a$ [nm]	$S_q$ [nm]	$S_z$ [ $\mu\text{m}$ ]	Surface Area/Project. Area
UNT	38	55.52	0.95	1.00
ULT	198±13	246±15	2.03±0.15	1.10
ULT25	285±19	359±33	3.15±0.8	1.16
ULT50	213±8	270±11	2.68±0.35	1.12
ULT75	242±13	302±11	2.11±0.1	1.10
ULT100	250±118*	316±145*	2.82±0.99	1.03

### 3.5 Diffusion bonding

For a preliminary evaluation of the manufacturing process chain, the joining between two untreated glasses was tested by diffusion bonding in oven. One sample was superimposed on another and they were placed in the oven with a weight of refractory material on top. After treatment at  $T_g+75^\circ\text{C}$  and  $T_g+100^\circ\text{C}$  it was seen that the two samples joined: it was not possible to separate them without breaking, as shown in Figure 10.

This could be a good starting point for the creation of devices.

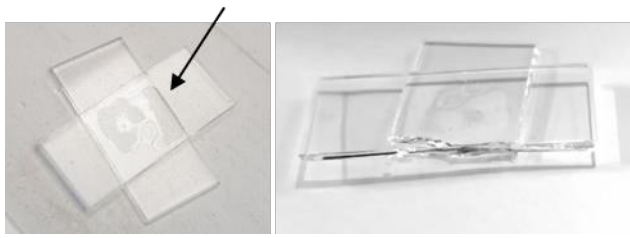


Figure 10. The bonded (left) and broken (right) samples

### 3.6 Complex geometries

To demonstrate the flexibility in the use of ultrafast laser micromanufacturing different complex geometries, typical of microfluidic devices were obtained, as visible in Figure 11. The images acquired by SEM, show the high accuracy that ultrafast lasers can achieve, unlike other traditional techniques: quasi-vertical sidewalls were obtained.

The Y channel is 100  $\mu\text{m}$  wide and 100  $\mu\text{m}$  deep, and was obtained at 500 mm/s of mark speed, filled with a 5  $\mu\text{m}$  spaced cross-etch fill.

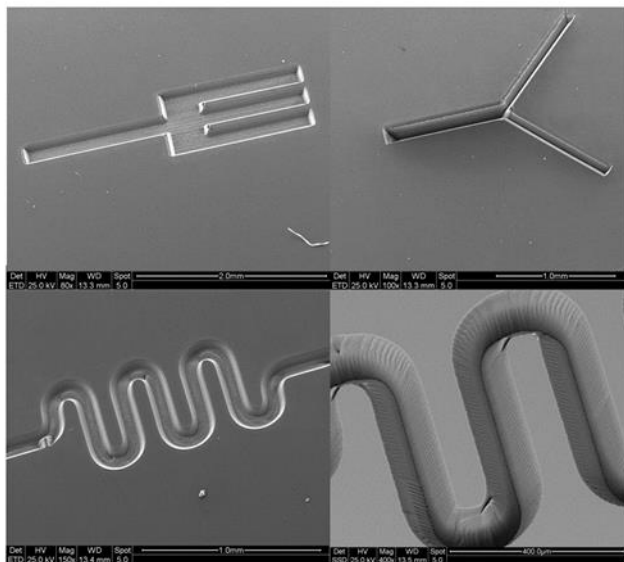


Figure 11. SEM images of the different complex geometries obtained

The fork channel is 200  $\mu\text{m}$  wide and about 100  $\mu\text{m}$  deep. Process time for the fork for example, made in 30 passes, is 180 s total.

## 4. Conclusion

It is increasingly important to find new technologies to fabricate microfluidic devices. In this work, the use of ultrashort laser micro-texturing has been evaluated for the rapid and precise prototyping of glass microfluidic devices. In addition, heat treatment above the glass transition temperature of a float-glass on both the hydrophilicity and the roughness of this material has been investigated.

It has been demonstrated that laser texturing increases the wettability of the studied material and thus its hydrophilicity. The hydrophilicity of laser textured material could be further enhanced by a heat treatment with a temperature up to 75  $^{\circ}\text{C}$  over the glass transition temperature. More than that, it is seen that even for a non-laser textured glass and with only a

heat treatment the material could achieve a super-hydrophilicity property. However, it is necessary to mention that for both untreated and laser textured glass, higher temperature treatment results in hydrophilicity decrease.

The roughness results are in accordance with those of wettability tests: it is found that the increasing of the heat treatment temperature leads to the decrease of the roughness.

On another side, the possibility to apply the diffusion bonding as manufacturing process has been demonstrated with heat treatment temperatures of 75  $^{\circ}\text{C}$  and 100  $^{\circ}\text{C}$  over the glass transition temperature, which could be a good starting point for the device creation.

For this reason, in a future work the proposed bonding method should be investigated by the evaluation of its capacity to withstand the pressure applied by the fluid inside the microchannels.

However, these results open interesting possibilities to create manufacturing process chain based on ultrashort laser and heat treatment for the prototyping and flexible production of glass microfluidic devices.

## References

- [1] Colombo S et al Transforming nanomedicine manufacturing toward Quality by Design and microfluidics. *Adv. Drug Deliv. Rev.* 2018; 128 115–131.
- [2] Zhang L et al Microfluidic Methods for Fabrication and Engineering of Nanoparticle Drug Delivery Systems. *ACS Appl. Bio Mater.* 2020; 3, 1 107–120.
- [3] Orazi L et al Ultrafast laser manufacturing: from physics to industrial applications. *CIRP Ann.* 2021; 70, 2 543–566.
- [4] Lee JN et al Solvent Compatibility of Poly(dimethylsiloxane)-Based Microfluidic Devices. *Anal. Chem.* 2003; 75, 23 6544–6554.
- [5] Adamiak W et al Compatibility of organic solvents for electrochemical measurements in PDMS-based microfluidic devices. *Microfluid. Nanofluidics* 2016; 20, 9 127.
- [6] Benson BR et al An “off-the-shelf” capillary microfluidic device that enables tuning of the droplet breakup regime at constant flow rates. *Lab. Chip* 2013; 13, 23 4507.
- [7] Wlodarczyk K et al Rapid Laser Manufacturing of Microfluidic Devices from Glass Substrates. *Micromachines* 2018; 9, 8 409.
- [8] Queste S et al Manufacture of microfluidic glass chips by deep plasma etching, femtosecond laser ablation, and anodic bonding. *Microsyst. Technol.* 2010; 16, 8 1485–1493.
- [9] Butkutė A, Jonušauskas L 3D Manufacturing of Glass Microstructures Using Femtosecond Laser. *Micromachines* 2021; 12, 5 499.
- [10] Sima F, Sugioka K Ultrafast laser manufacturing of nanofluidic systems. *Nanophotonics* 2021; 10, 9 2389–2406.
- [11] Owusu-Ansah E, Dalton C Fabrication of a 3D Multi-Depth Reservoir Micromodel in Borosilicate Glass Using Femtosecond Laser Material Processing. *Micromachines* 2020; 11, 12 1082.
- [12] Wlodarczyk KL et al Maskless, rapid manufacturing of glass microfluidic devices using a picosecond pulsed laser. *Sci. Rep.* 2019; 9, 1 20215.
- [13] Chang T-L et al Effect of ultra-fast laser texturing on surface wettability of microfluidic channels. *Microelectron. Eng.* 2012; 98 684–688.
- [14] Camli B et al Rapid prototyping of noncontact microwave microfluidic devices for sensing applications. *J. Micromechanics Microengineering* 2021; 31, 9 097001.
- [15] Li W et al A three-dimensional microfluidic mixer of a homogeneous mixing efficiency fabricated by ultrafast laser internal processing of glass. *Appl. Phys. A* 2020; 126, 10 816.
- [16] Pan Y-J, Yang R-J A glass microfluidic chip adhesive bonding method at room temperature. *J. Micromechanics Microengineering* 2006; 16, 12 2666–2672.
- [17] Liu Y et al Bench scale glass-to-glass bonding for microfluidic prototyping. *Microsyst. Technol.* 2020; 26, 12 3581–3589.